

# ParisKV: Fast and Drift-Robust KV-Cache Retrieval for Long-Context LLMs

Yanlin Qi<sup>1</sup> Xinhang Chen<sup>2</sup> Huiqiang Jiang<sup>3</sup> Qitong Wang<sup>4</sup> Botao Peng<sup>5</sup> Themis Palpanas<sup>1</sup>

## Abstract

KV-cache retrieval is essential for long-context LLM inference, yet existing methods struggle with distribution drift and high latency at scale. We introduce ParisKV, a drift-robust, GPU-native KV-cache retrieval framework based on collision-based candidate selection, followed by a quantized inner-product reranking estimator. For million-token contexts, ParisKV supports CPU-offloaded KV caches via Unified Virtual Addressing (UVA), enabling on-demand top- $k$  fetching with minimal overhead. ParisKV matches or outperforms full attention quality on long-input and long-generation benchmarks. It achieves state-of-the-art long-context decoding efficiency: it matches or exceeds full attention speed even at batch size 1 for long contexts, delivers up to  $2.8\times$  higher throughput within full attention’s runnable range, and scales to million-token contexts where full attention runs out of memory. At million-token scale, ParisKV reduces decode latency by  $17\times$  and  $44\times$  compared to MagicPIG and PQCache, respectively, two state-of-the-art KV-cache Top- $k$  retrieval baselines.

## 1. Introduction

Large language models (LLMs) (Achiam et al., 2023; Touvron et al., 2023; Jiang et al., 2023; Yang et al., 2025) are rapidly extending their context windows to millions of tokens, placing unprecedented pressure on inference efficiency. The KV-cache, which stores keys and values of all preceding tokens for autoregressive decoding, quickly dominates both memory footprint and latency as context grows (Zhang et al., 2023; Li et al., 2024; Chen et al., 2024). Crucially, long-context decoding is memory-bound: each step requires reading a large volume of KV vectors, and bandwidth cost scales linearly with context length. This

<sup>1</sup>LIPADE, Université Paris Cité, Paris, France <sup>2</sup>Xi'an Jiaotong University, Xi'an, China <sup>3</sup>Microsoft Research, Shanghai, China <sup>4</sup>Harvard University, Cambridge, MA, USA <sup>5</sup>Institute of Computing Technology, Chinese Academy of Sciences, Beijing, China. Correspondence to: Botao Peng <pengbotao@ict.ac.cn>.

Preprint. February 10, 2026.

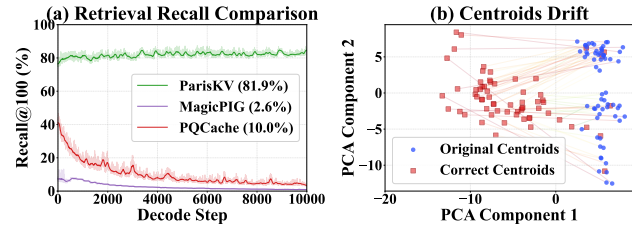


Figure 1. Retrieval drift results. (a) Recall comparison of different methods on AIME. (b) Centroid drift induced by decoding keys, measured as the mismatch between *prefill-only* centroids (original centroids in blue) and *reference* centroids (correct centroids in red) obtained by clustering all keys from both prefill and decoding.

has motivated sparse/selective attention, which exploits the empirical sparsity of attention by attending only to a Top- $k$  subset of relevant past tokens.

Among sparse designs, KV-cache dropping/eviction methods permanently discard tokens and can be brittle when early tokens become critical later. In contrast, KV-cache retrieval retains the full KV history and dynamically retrieves relevant keys at each step, making it better suited for open-ended long-context inference.

**Challenges:** Despite its accuracy advantages, KV-cache retrieval faces the following efficiency challenges in latency-sensitive, long-generation scenarios. (C1) Speed-quality tradeoff: Lightweight approximate retrieval (e.g., coarse clustering, low-bit quantization) sacrifices recall for speed; recovering accuracy requires increasing the retrieval budget, eroding the benefits of sparsity. (C2) Decoding drift: Centroids learned from clustering prefill keys become stale as generation continues. Figure 1(a) shows an example, where prior methods (Zhang et al., 2025; Chen et al., 2024) suffer severe recall collapse during long decoding, while ParisKV maintains stable recall. Figure 1(b) visualizes the root cause: prefill-only centroids (in blue) increasingly mismatch the true key distribution (in red) as decode keys accumulate. (C3) CPU-bound retrieval and data movement: When the full KV cache is offloaded to CPU memory, retrieval typically involves CPU-side search and CPU-to-GPU data transfer. The GPU can only access representations (centroids or low-bit codes), which introduce approximation errors, while CPU orchestration dominates end-to-end latency.

**Our approach.** We present ParisKV, a hardware-aware algorithm–system co-design for KV-cache retrieval that

achieves fast decoding, stable recall under long input and/or long-generation (i.e., million-token scalability), even in the presence of drift.

Unlike prior methods that learn centroids from prefill keys, ParisKV transforms queries and keys into a stable, data-independent space by normalizing them onto the unit hypersphere (see Fig. 3) and applying a shared random orthogonal rotation, where we can analytically define a set of uniformly distributed centroids. These centroids are uniformly distributed on the unit hypersphere (see Fig. 3), so any newly generated keys will always be close to at least one centroid. In this way, ParisKV avoids stale centroids (i.e., centroids that become mismatched during decoding), and maintains stable retrieval quality throughout long generations.

ParisKV adopts a two-stage pipeline implemented entirely on GPU. The coarse stage uses multi-subspace collision counting to aggressively prune candidates; the fine stage reranks them using calibrated inner-product estimates from compact representation of original keys, achieving high recall without accessing full-precision keys on CPU.

Moreover, ParisKV offloads the full KV cache to CPU memory and leverages Unified Virtual Addressing (UVA) to let GPU kernels directly fetch only the selected Top- $k$  KV pairs on demand, bypassing explicit memcpy and CPU-side scheduling overhead.

**Contributions.** (1) We propose drift-robust analytic centroids, a data-independent transformation that maintains stable retrieval recall even under significant distribution shift at the million-token scale. (2) We design a GPU-native coarse-to-fine retrieval pipeline combining collision-based pruning and calibrated reranking, achieving high-fidelity Top- $k$  selection directly on compressed codes without CPU-side search. (3) We implement a scalable UVA-based offloading system enabling on-demand KV fetching with minimal CPU intervention. (4) Extensive evaluations show ParisKV delivers up to 17 $\times$  and 45 $\times$  speedups over MagicPIG and PQCache at 1M-token scale, while maintaining near-lossless quality on long-input and long-form reasoning benchmarks.

## 2. Related Work

### 2.1. KV-Cache Quantization

Several recent studies have proposed innovative methods to tackle the challenges of KV-Cache quantization while keeping performance degradation minimal.

Quantization-friendly transformations reduce quantization difficulty via offline distribution reshaping. SmoothQuant (Xiao et al., 2023a) enables 8-bit KV-Cache quantization, while QuaRot, QuQuant, and SpinQuant further suppress outliers through randomized or learnable transformations (Ashkboos et al., 2024; Lin et al., 2024; Liu et al., 2024c).

Sparsity-aware quantization combines importance modeling with low-bit quantization; Q-Hitter (Zhang et al., 2024) leverages attention statistics to jointly apply sparsity and 8-bit quantization. Structure-aware and mixed-precision quantization exploits KV heterogeneity via offline tuning: KIVI (Liu et al., 2024b) applies asymmetric quantization for 2-bit compression, while KV Tuner (Li et al., 2025) determines layer-wise mixed-precision configurations.

### 2.2. Sparse KV-Cache

Sparse KV-Cache methods reduce the memory and computation cost of long-context inference by exploiting attention sparsity. Existing work can be broadly categorized into *KV-Cache Dropping* and *KV-Cache Retrieval*.

**KV-Cache Dropping.** KV-Cache Dropping permanently removes KV entries that are predicted to be unimportant. StreamingLLM (Xiao et al., 2023b) treats early tokens as sinks, while H2O (Zhang et al., 2023), SnapKV (Li et al., 2024), Keyformer (Adnan et al., 2024), and Expected Attention (Devoto et al., 2025) estimate token importance from attention statistics. KeyDiff (Park et al., 2025) infers importance from key diversity, enabling compatibility with optimized attention implementations (Dao et al., 2022; Dao, 2023). Structure-aware methods further exploit head and layer-level heterogeneity, including DuoAttention (Xiao et al., 2024), PyramidKV (Cai et al., 2024), AdaKV (Feng et al., 2024), and HeadKV (Fu et al., 2024). KVZip (Kim et al., 2025) identifies important historical KV entries via offline reconstruction.

**KV-Cache Retrieval.** KV-Cache Retrieval dynamically selects a small subset of KV entries per step without permanently removing them. Pattern-aware sparse attention mainly targets the prefill stage, including MInference (Jiang et al., 2024), FlexPrefill (Lai et al., 2025), XAttention (Xu et al., 2025), and SeerAttention (Gao et al., 2024). Decode-stage retrieval is explored by Quest (Tang et al., 2024), while MoBA (Lu et al., 2025) and NSA (Yuan et al., 2025) integrate retrieval mechanisms into training. CPU-assisted retrieval further extends effective KV capacity, such as MagicPig (Chen et al., 2024), PQCache (Zhang et al., 2025), RetroInfer (Chen et al., 2025), ShadowKV (Sun et al., 2024), and RetrievalAttention (Liu et al., 2024a).

## 3. Background and Problem Formulation

We study *KV-cache retrieval* for accelerating autoregressive decoding in Transformers. At decoding step  $t$ , each attention head issues a query vector  $\mathbf{q} \in \mathbb{R}^D$ , and attends to a growing set of keys  $\mathcal{K} = \{\mathbf{k}_i \in \mathbb{R}^D\}_{i=1}^{n_t}$  with corresponding values  $\mathcal{V} = \{\mathbf{v}_i\}_{i=1}^{n_t}$  stored in the KV cache. The pre-softmax attention score between a key and the query is  $s(\mathbf{k}_i, \mathbf{q}) \triangleq$

$\langle \mathbf{k}_i, \mathbf{q} \rangle$ . In exact attention, we compute a softmax over *all* cached keys and aggregate values:

$$\alpha_i(\mathbf{q}) = \frac{\exp(s(\mathbf{k}_i, \mathbf{q}))}{\sum_{j=1}^{n_t} \exp(s(\mathbf{k}_j, \mathbf{q}))}, \quad \mathbf{o}(\mathbf{q}) = \sum_{i=1}^{n_t} \alpha_i(\mathbf{q}) \mathbf{v}_i. \quad (1)$$

However, the KV cache grows with  $t$ , making Eq. (1) increasingly expensive.

**Top- $k$  retrieval for approximate attention.** To reduce latency, we aim to retrieve only the top- $k$  keys with the largest inner products:  $\text{TopK}(\mathbf{q}) \triangleq \arg \max_{i \in [n_t]}^k \langle \mathbf{k}_i, \mathbf{q} \rangle$ . Given a small candidate set  $\mathcal{C}(\mathbf{q}) \subseteq [n_t]$  (ideally containing  $\text{TopK}(\mathbf{q})$ ), we compute *approximate attention* by restricting the softmax to  $\mathcal{C}(\mathbf{q})$ :

$$\tilde{\alpha}_i(\mathbf{q}) = \frac{\exp(s(\mathbf{k}_i, \mathbf{q}))}{\sum_{j \in \mathcal{C}(\mathbf{q})} \exp(s(\mathbf{k}_j, \mathbf{q}))}, \quad i \in \mathcal{C}(\mathbf{q}). \quad (2)$$

$$\tilde{\mathbf{o}}(\mathbf{q}) = \sum_{i \in \mathcal{C}(\mathbf{q})} \tilde{\alpha}_i(\mathbf{q}) \mathbf{v}_i. \quad (3)$$

When  $\mathcal{C}(\mathbf{q})$  covers the true top- $k$  keys, Eq. (3) closely matches the exact output in Eq. (1) while being faster.

## 4. The ParisKV Framework

ParisKV is an algorithm–system co-design for fast long-context decoding with *drift-robust* retrieval. We first provide an overview of ParisKV, and then discuss the details.

In the *prefill* phase (refer to Fig. 2), beyond computing the KV cache, ParisKV performs a one-time *key summarization* to enable fast on-device retrieval during decoding. Specifically, we (i) apply a shared normalization-and-rotation transform to make representations stable under decoding drift, and (ii) build compact per-key metadata that stays on GPU after the full-precision KV cache is offloaded to CPU. These metadata have two parts. First, we use a small *codebook*, i.e., a small set of centroid IDs that summarize keys (A.2 in Fig. 2), which is later used to quickly generate candidates via collision-based voting (B.2.1 in Fig. 2). Second, we store a compact quantized code per subspace for each key (A.3.1), together with a lightweight scaling factor for calibration (A.3.2). These quantized codes and scaling factors are then used to efficiently estimate query–key inner products and rerank candidates (B.2.2) without accessing full-precision keys on GPU. Overall, prefill produces small, GPU-resident summaries for retrieval, while the full-precision KV cache is asynchronously offloaded to CPU memory to allow scalability to long contexts.

In the *decode* phase (refer to Fig. 2 and Fig. 4), ParisKV uses a two-step retrieval pipeline. (1) Coarse Candidate Generation (B.2.1) narrows the search space using only lightweight GPU-resident *codebook* summaries. For a query, we select the few most similar centroids in each subspace; keys

in these selected buckets receive one vote. We sum votes across subspaces and keep the high-vote keys as candidates. (2) Candidate Reranking reranks the candidates generated earlier by estimating their query–key inner products and selecting the final Top- $k$  keys for attention. During this step, the GPU maintains compact 4-bit quantized codes of the keys, but cannot (efficiently) access the full-precision raw vectors, which are in the CPU memory. Thus, ParisKV computes a fast, subspace-wise inner-product estimate using the quantized codes and corrects the quantization error using a lightweight procedure (see Fig. 4 bottom), achieving high fidelity, and consequently enabling high-recall in the Top- $k$  selection. Estimating the query–key inner products involves many fine-grained operations, so we implement a *reranking fused kernel* to streamline the computation.

### 4.1. Prefill Phase

#### 4.1.1. PREPROCESSING

ParisKV applies a shared normalize–rotate transform, splits vectors into rotated subspaces, and uses a polar (radius–direction) form to summarize each subspace (A.1 in Fig. 2). Given prefill keys  $\{\mathbf{k}_i\}_{i=1}^n$ , ParisKV constructs compact per-key metadata on GPU (queries are processed in the same way). It proceeds as follows.

**(1) Normalize & rotate.** Normalization maps all keys and queries onto the same unit-hypersphere space, so similarity comparisons depend only on direction (not magnitude). The shared rotation spreads information more evenly across dimensions while preserving inner products, making later bucketing and scoring more stable under drift. We first  $\ell_2$ -normalize keys and queries:  $\hat{\mathbf{k}}_i = \frac{\mathbf{k}_i}{\|\mathbf{k}_i\|_2}$ ,  $\hat{\mathbf{q}} = \frac{\mathbf{q}}{\|\mathbf{q}\|_2}$ .

We then apply a shared orthogonal rotation  $\mathbf{R}$  (implemented by SRHT):  $\tilde{\mathbf{k}}_i = \mathbf{R}\hat{\mathbf{k}}_i$ ,  $\tilde{\mathbf{q}} = \mathbf{R}\hat{\mathbf{q}}$ . Since  $\mathbf{R}$  is orthogonal, it preserves inner products:  $\langle \tilde{\mathbf{k}}_i, \tilde{\mathbf{q}} \rangle = \langle \hat{\mathbf{k}}_i, \hat{\mathbf{q}} \rangle$ .

*Example.* Assume  $m = 3$ . Then, the codebook has  $2^3 = 8$  direction centers:  $\Omega = \left\{ \left( \pm \frac{1}{\sqrt{3}}, \pm \frac{1}{\sqrt{3}}, \pm \frac{1}{\sqrt{3}} \right) \right\}$ ,  $|\Omega| = 8$ . These 8 centers correspond to the 8 corners of a cube. After scaling to unit norm, they lie on the unit sphere and evenly cover the 8 “octants” (i.e., eight coarse directions in 3D space). Given a rotated key  $\tilde{\mathbf{k}}$ , we simply assign it to the nearest center in  $\Omega$ . For instance, if  $\tilde{\mathbf{k}}$  points roughly to the “ $(+, +, -)$ ” direction, it will be assigned to  $\left( \frac{1}{\sqrt{3}}, \frac{1}{\sqrt{3}}, -\frac{1}{\sqrt{3}} \right)$ . (The details are shown in Fig. 3)

**(2) Subspace split.** Subspace splitting enables efficient parallel processing and provides multiple independent votes for our collision-based candidate filtering. We partition  $\tilde{\mathbf{k}}_i$  (and  $\tilde{\mathbf{q}}$ ) into  $B$  contiguous subspaces of dimension  $m = D/B$ :  $\tilde{\mathbf{k}}_i = [\tilde{\mathbf{k}}_{i,1}; \dots; \tilde{\mathbf{k}}_{i,B}]$  and  $\tilde{\mathbf{q}} = [\tilde{\mathbf{q}}_1; \dots; \tilde{\mathbf{q}}_B]$ , where  $\tilde{\mathbf{k}}_{i,b}, \tilde{\mathbf{q}}_b \in \mathbb{R}^m$ .

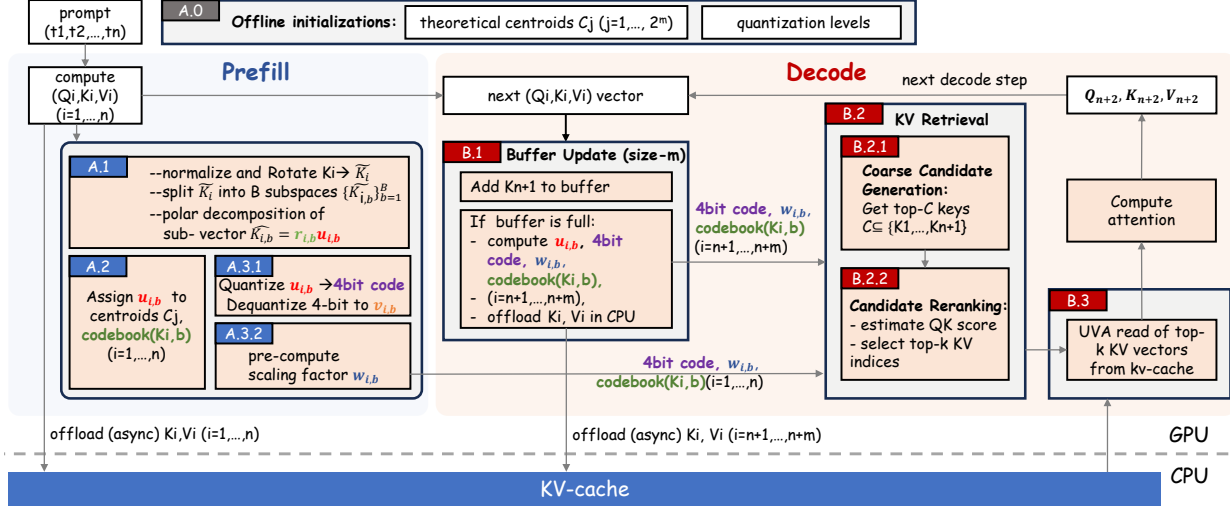


Figure 2. ParisKV pipeline. Offline, we construct an analytic centroid codebook and a quantization configuration. During prefill, we materialize the KV cache and build GPU-resident key summaries (centroid IDs for Stage-I vote-based filtering, and low-bit codes with lightweight weights for Stage-II reranking), while asynchronously offloading full-precision KV to CPU memory. During decoding, summaries for newly generated keys are incrementally updated; the GPU performs coarse-to-fine retrieval (voting → reranking) using only these summaries, then fetches the selected Top- $k$  KV pairs from CPU via UVA for attention.

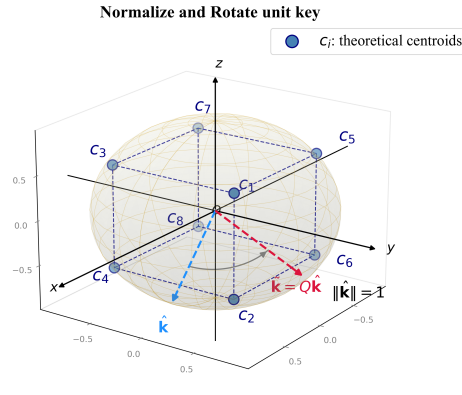


Figure 3. Illustration of rotation-based codebook assignment on the unit sphere.

**(3) Polar decomposition.** Polar form further separates direction (for voting) from radius (for calibrated inner-product estimation). For each key  $i$  and subspace  $b$ , define  $r_{i,b} = \|\tilde{\mathbf{k}}_{i,b}\|_2$  and  $\mathbf{u}_{i,b} = \tilde{\mathbf{k}}_{i,b}/r_{i,b}$ , so that  $\tilde{\mathbf{k}}_{i,b} = r_{i,b}\mathbf{u}_{i,b}$  (similarly for  $\tilde{\mathbf{q}}_b$ ). This yields an additive subspace form of the rotated inner product:

$$\langle \tilde{\mathbf{k}}_i, \tilde{\mathbf{q}} \rangle = \sum_{b=1}^B \langle \tilde{\mathbf{k}}_{i,b}, \tilde{\mathbf{q}}_b \rangle = \sum_{b=1}^B r_{i,b} \langle \mathbf{u}_{i,b}, \tilde{\mathbf{q}}_b \rangle. \quad (4)$$

#### 4.1.2. ASSIGN DIRECTIONS TO CENTROIDS

We map each  $\mathbf{u}_{i,b}$  to its nearest direction centroid  $\mathbf{c}_j$  (A.2 in Fig. 2), and store the centroid ids codebook to use during decoding for the collision-based candidate generation.

**Data-independent uniform direction centroids.** After  $\ell_2$  normalization and SRHT rotation, subspace directions

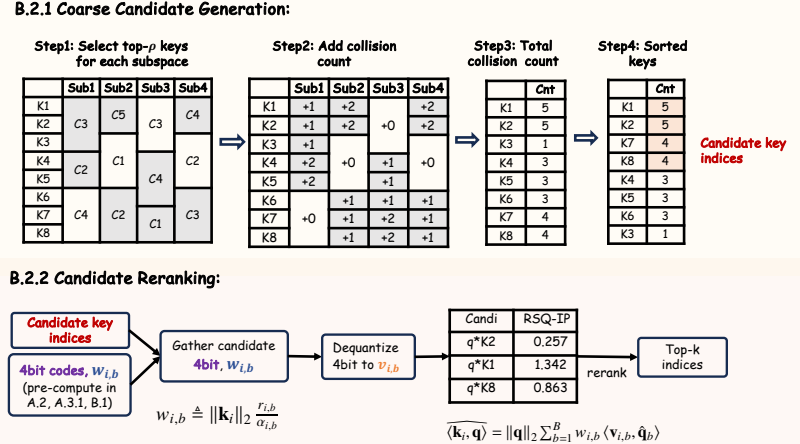


Figure 4. ParisKV Retrieval algorithm (shown as B.2 in Fig. 2)

become approximately isotropic, making it effective to use a *shared, data-independent* set of direction centroids instead of learning them from data. Thus, in each  $m$ -dimensional subspace we predefine a sign-pattern centroid set

$$\Omega \triangleq \left\{ \pm \frac{1}{\sqrt{m}} \right\}^m, \quad |\Omega| = 2^m, \quad (5)$$

where each  $\omega \in \Omega$  is a unit direction with equal-magnitude coordinates. Given a subspace unit direction  $\mathbf{u}_{i,b}$ , we assign it to the nearest centroid in  $\Omega$  and store the resulting index

$$\text{centroid\_id}_{i,b} \triangleq \arg \max_{\omega \in \Omega} \langle \mathbf{u}_{i,b}, \omega \rangle. \quad (6)$$

#### 4.1.3. A.3 LOW-BIT RERANK METADATA

To rerank candidates without accessing full-precision keys in CPU memory, we store lightweight per-subspace sum-

marries on-GPU: (A.3.1) a 4-bit direction code  $\text{code}_{i,b}$  that dequantizes to a reconstructed direction  $\mathbf{v}_{i,b}$ , and (A.3.2) a scalar weight  $w_{i,b}$  that precomputes all key-only factors during candidate reranking. Specifically, with subspace radius  $r_{i,b} = \|\tilde{\mathbf{k}}_{i,b}\|_2$  and per-subspace correction term

$$\alpha_{i,b} \triangleq \langle \mathbf{v}_{i,b}, \mathbf{u}_{i,b} \rangle. \quad (7)$$

where  $\mathbf{u}_{k,b}$  is the (unknown) true unit direction of key  $k$  in subspace  $b$  and  $\mathbf{v}_{k,b}$  is its quantized direction. Intuitively,  $\alpha_{k,b}$  measures the alignment between the quantized direction and the true direction; quantization typically shrinks this alignment, causing a systematic underestimation of the query–key inner product if we directly use  $\langle \mathbf{v}_{k,b}, \tilde{\mathbf{q}}_b \rangle$ . Specifically, our reranking estimator employs the approximation

$$\langle \mathbf{u}_{k,b}, \tilde{\mathbf{q}}_b \rangle \approx \frac{\langle \mathbf{v}_{k,b}, \tilde{\mathbf{q}}_b \rangle}{\alpha_{k,b}}, \quad (8)$$

we define a per-key, per-subspace scaling factor

$$w_{i,b} \triangleq \|\mathbf{k}_i\|_2 \frac{r_{i,b}}{\alpha_{i,b}}. \quad (9)$$

Notably,  $w_{i,b}$  depends only on the key and the quantization metadata, and does *not* involve the query. Therefore, it can be precomputed once during the prefill stage and cached, so that online reranking only computes lightweight dot products between the quantized direction and the rotated query, and then rescales them using the cached  $w_{i,b}$  to estimate  $\langle \mathbf{k}_i, \mathbf{q} \rangle$  efficiently. Online reranking then becomes a simple weighted accumulation over subspaces:

$$\widehat{\langle \mathbf{k}_i, \mathbf{q} \rangle} = \|\mathbf{q}\|_2 \sum_{b=1}^B w_{i,b} \langle \mathbf{v}_{i,b}, \tilde{\mathbf{q}}_b \rangle. \quad (10)$$

Overall, prefill stores metadata  $\{(\text{centroid\_id}_{i,b}, \text{code}_{i,b}, w_{i,b})\}_{i \leq n, b \leq B}$  on GPU, while full-precision  $(\mathbf{k}_i, \mathbf{v}_i)$  are kept in CPU memory for on-demand UVA fetching.

## 4.2. Decode Phase

### 4.2.1. BUFFER UPDATE

As decoding proceeds, we maintain the KV-cache as four contiguous regions (Fig. 5): *Sink* (a small set of early high-attention tokens kept on GPU), *Retrieval* (offloaded and indexed historical tokens), *Local* (the most recent local\_size tokens kept on GPU for dense attention), and *Update Buffer* on GPU that temporarily holds newly generated tokens.

We append each new token to the Update Buffer (B.1 in Fig. 2). When the buffer reaches  $m$  tokens, we trigger a sliding-window update: (i) the oldest  $m$  tokens in the Local region are evicted into the Retrieval region (via GPU→CPU transfer in the offload setting); (ii) the Local window is shifted to keep the most recent local\_size tokens by promoting the buffered tokens into Local (and clearing the

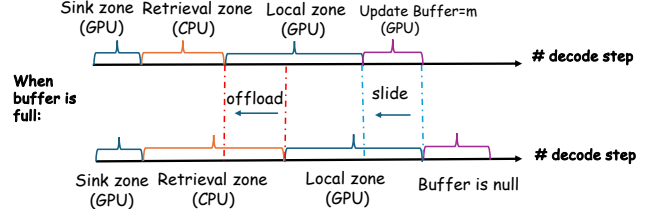


Figure 5. Sliding-window KV-cache update.

buffer); and (iii) we encode and index the evicted keys on GPU (centroid ids, 4-bit codes, and  $w_{i,b}$ ), while offloading the corresponding full-precision KV pairs asynchronously. This streaming update supports unbounded generation while keeping retrieval metadata fresh and preserving fast access to both recent context (Local) and long-range history (Retrieval).

### 4.2.2. RETRIEVAL

At each decoding step, ParisKV performs a fully on-GPU two-step retrieval pipeline (Fig. 4 and B.2 in Fig. 2) to approximate Top- $k$  attention selection without accessing full-precision keys during ranking.

**(1) Coarse candidate generation** (B.2.1). We use a direction-only proxy to quickly prune the full key set to a small candidate pool. Concretely, we decompose the rotated key/query into  $B$  subspaces and score each key by accumulating subspace-wise collision bonuses: in each subspace we compare the query to the key’s assigned centroid (cheap dot product  $q^\top c$ ) and only let the top- $\rho$  fraction contribute a non-zero bonus. Summing across subspaces yields a coarse integer score that is robust to decoding drift and enables fast pruning to the top- $\beta$  fraction as candidates (typically  $\beta=5\%-10\%$ ). We set  $\rho \geq \beta$  so each subspace contributes sufficiently many non-zero terms, and the candidate pool remains comfortably larger than the final Top- $k$  (e.g.,  $k=100$ ) used in reranking. We use an adaptive schedule of  $(\rho, \beta)$  w.r.t. KV length.

**(2) Candidate Reranking** (B.2.2). We rerank candidates by estimating the raw attention score  $\langle \mathbf{k}, \mathbf{q} \rangle$  directly from compact 4-bit key quantizations. Each subspace direction is encoded with *1-bit sign + 3-bit magnitude* per coordinate. Online reranking only computes lightweight dot products between the quantized direction and the rotated query, combined with a precomputed per-subspace scaling factor. This yields an accurate estimator of raw inner products while avoiding any access to full-precision keys during reranking. Full-precision KV are fetched *only* for the final selected Top- $k$  tokens. The derivation of the theoretical quantization levels for the normalized-and-rotated subspace directions is guided by Proposition 4.1.

**Proposition 4.1** (Rotation-induced Beta priors for subspaces). *Let  $\hat{\mathbf{k}} \in \mathbb{S}^{D-1}$  be any unit vector and  $\mathbf{R} \in \mathbb{R}^{D \times D}$  be Haar-random orthogonal. Let  $\tilde{\mathbf{k}} = \mathbf{R}\hat{\mathbf{k}}$  and partition it*

into  $B$  contiguous subspaces of dimension  $m$  ( $D = Bm$ ):  $\mathbf{k} = [\tilde{\mathbf{k}}_1; \dots; \tilde{\mathbf{k}}_B]$ .

Define  $r_b = \|\tilde{\mathbf{k}}_b\|_2$ ,  $z_b = r_b^2 \in [0, 1]$ , and  $\mathbf{u}_b = \tilde{\mathbf{k}}_b/r_b \in \mathbb{S}^{m-1}$ . Here,  $z_b$  is the subspace energy fraction (squared radius) after polar decomposition, which we use to design radius quantization centroids (Eq. (11));  $\mathbf{u}_b$  is the corresponding unit direction within subspace  $b$ , whose coordinate-wise distribution in Eq. (12) guides the design of quantization levels for the normalized-and-rotated representation. Then for any fixed  $b \in [B]$  and  $j \in [m]$ :

$$z_b \sim \text{Beta}\left(\frac{m}{2}, \frac{D-m}{2}\right), \quad (11)$$

$$(\mathbf{u}_b)_j^2 \sim \text{Beta}\left(\frac{1}{2}, \frac{m-1}{2}\right). \quad (12)$$

**Implementation.** Both stages are realized with custom CUDA kernels: (i) a collision accumulation kernel and a small-range integer *bucket\_topk* kernel for Top- $\beta$  selection, and (ii) a fused reranking kernel for RSQ-IP.

#### 4.2.3. ON-DEMAND UVA FETCH

Finally, the GPU fetches only the selected Top- $k$  KV pairs from CPU memory via UVA, and computes attention (B.3 in Fig. 2). Thus, CPU memory serves as a backing store for capacity, while the retrieval decision path remains GPU-native.

### 4.3. Implementation Optimizations and Complexity

ParisKV relies on a coarse-to-fine retrieval pipeline whose latency is dominated by GPU selection, reranking, and KV fetching. We implement four custom CUDA kernels to eliminate sorting overhead, reduce kernel launches, and minimize memory traffic: (i) *bucket\_topk* for integer collision scores, (ii) a parallel collision kernel, (iii) a fused reranking kernel (gather+unpack+score), and (iv) a UVA-based kernel.

**Complexity.** Let  $|S|$  be the on-GPU steady/local attention length and  $n = |R|$  the retrieval-zone length. Dense scoring over the full cache scales with  $\mathcal{O}((|S|+n)D)$  per step. ParisKV keeps dense attention only on  $|S|$  and replaces full-cache scoring with a coarse-to-fine pipeline on compact metadata: collision processing scales with  $\rho n$ , reranking scales with  $C = \lceil \beta n \rceil$ , and only  $k \ll C$  KV vectors are fetched for attention.

## 5. Experimental Evaluation

We evaluate ParisKV on long-generation reasoning (MATH500 (Hendrycks et al., 2021), GPQA-Diamond (Rein et al., 2024), AIME25 (Balunović et al., 2025)) and long-context understanding (LongBench-V2 (Bai et al., 2024)) across three model families (Qwen-3-8B (Qwen Team, 2025), DeepSeek-R1-Llama-8B (Guo et al., 2025),

Table 1. Hyperparameter configurations across different tasks.

Dataset	Local	Update	Full-thres.	Max Gen
AIME25	256	512	2K	38.9K
MATH500	256	256	1K	38.9K
GPQA-Diamond	128	512	2K	32.8K
LongBench_V2	256	512	2K	1024+512

Methods	GPQA_dia (pass@1)	MATH500 (pass@1)	AIME_2025 (pass@8)
<i>Qwen-3-4B</i>	64.14	88.60	<b>86.67</b>
PQCache	38.38	58.80	3.33
MagicPIG	32.32	46.40	6.67
<b>ParisKV (Ours)</b>	<b>72.22</b>	<b>92.80</b>	<b>80.00</b>
<i>DS-R1-Llama-8B</i>	49.49	80.40	50.00
PQCache	23.81	66.75	13.30
MagicPIG	27.78	49.00	13.30
<b>ParisKV (Ours)</b>	<b>57.07</b>	<b>84.40</b>	<b>53.30</b>
<i>Qwen-3-8B</i>	54.54	87.40	<b>83.33</b>
PQCache	47.85	69.21	16.67
MagicPIG	33.84	45.80	10.00
<b>ParisKV (Ours)</b>	<b>55.05</b>	<b>93.00</b>	<b>73.33</b>

Table 2. Accuracy on long-generation tasks: GPQA\_diamond (pass@1), MATH500 and AIME\_2025 (pass@8).

and Qwen3-4B-Thinking-2507 (Qwen Team, 2025)). For fair comparison, we keep the KV-cache configuration in Table 1 consistent across methods. In all experiments, ParisKV uses a *fixed* retrieval budget of  $\text{top-}K=100$ , while PQCache (Zhang et al., 2025) and MagicPIG (Chen et al., 2024) follow their paper-recommended *budget policies* (PQCache uses 20% compress ratio and MagicPIG uses a dynamic retrieval policy whose effective retrieval size varies with sequence length).

#### 5.1. Accuracy evaluation

We evaluate ParisKV on both long-generation reasoning benchmarks and long-context understanding tasks. Across all settings, ParisKV improves accuracy over prior KV-cache retrieval baselines.

**Long-generation tasks.** Table 2 reports results on GPQA-Diamond (pass@1), MATH500 (pass@1), and AIME25 (pass@8) across three model families. ParisKV consistently outperforms PQCache and MagicPIG, and in 7/9 settings it even **matches or exceeds** full-attention accuracy.

On *Qwen-3-4B*, it achieves 72.22 (GPQA-Diamond) and 92.80 (MATH500), exceeding PQCache by +33.84 and +34.00 points.

**Long-input tasks.** We evaluate long-context understanding on LongBench-V2 (w/ CoT). ParisKV consistently improves accuracy over PQCache and MagicPIG, with the strongest gains in the Medium/Long buckets. For example, on DeepSeek-R1-Llama-8B, ParisKV increases the overall score to 28.43 (vs. 19.90 for PQCache and 13.92 for MagicPIG) and achieves 31.11 (Easy) / 30.16 (Hard) on Long inputs (Table 3).

**Summary.** ParisKV improves accuracy in both *long-generation* reasoning and *long-input* understanding settings. Compared to long-generation benchmarks, long-input tasks are typically less prone to retrieval drift because decoding produces far fewer tokens than the prefill length, leaving fewer opportunities for approximation errors to accumulate. Even in this easier regime, ParisKV still consistently outperforms prior KV-cache retrieval baselines on LONGBENCH-V2, including in the Medium/Long buckets. The gains become substantially larger in long-generation reasoning, where drift can compound over tens of thousands of decoding steps: on AIME25, ParisKV improves pass@8 by +40.0 to +76.7 points over PQCache/MagicPIG across model families (Table 2). Overall, these results indicate that ParisKV is robust across long-context regimes, and is especially effective when the decoding horizon is long and retrieval errors would otherwise accumulate.

## 5.2. Efficiency evaluation

We evaluate ParisKV’s decoding efficiency under varying context lengths and batch sizes, compare end-to-end latency and report the overhead of the prefilling stage. ParisKV achieves strong efficiency and scalability for long-context inference.

(1) Better batch scaling. Across 64K/128K/256K contexts, ParisKV improves the peak decoding throughput over full attention by  $2.1 \times \sim 2.8 \times$  on both Llama3.1-8B and Qwen3-8B (up to  $2.7 \times$  on Llama3.1-8B and  $2.8 \times$  on Qwen3-8B). Moreover, ParisKV sustains significantly larger runnable batch sizes where full attention becomes memory-bounded (e.g., at 128K full attention OOMs at  $bs \geq 4$  while ParisKV scales to  $bs=8$ ; at 256K full attention OOMs at  $bs \geq 2$  while ParisKV scales to  $bs=5$ ).

(2) Stable decoding latency. ParisKV exhibits smooth TPOT scaling with batch size. For example, on Qwen3-8B at 128K, TPOT increases from 24.32ms/step ( $bs=1$ ) to 58.92ms/step ( $bs=8$ ), reducing per-token latency from 24.32ms/token to 7.37 ms/token due to amortization.

(3) Superior performance at extremely long contexts. When full attention becomes infeasible (OOM at 384K even with  $bs=1$ ), ParisKV remains runnable and scales up to  $bs=3$ . Under 128K~1024K ( $bs=1$ ), ParisKV substantially outperforms representative KV-retrieval baselines. On Llama3.1-8B, ParisKV achieves up to  $44.4 \times$  lower decode latency than PQCache (e.g., 49ms/step vs. 2179ms/step at 1024K), and also significantly outperforms MagicPIG with up to  $16.9 \times$  lower decode latency at 1024K (49ms/step vs. 830ms/step). Similar trends hold for Qwen3-8B, where ParisKV consistently maintains decoding latency in the tens-of-milliseconds range while MagicPIG and PQCache incur substantially higher per-step overheads at long contexts.

## 5.3. Ablation Studies

**(1) Drift mitigation with normalization/rotation + theoretical spherical centroids.** This design substantially improves coarse-stage candidate generation under long decoding and translates into large end-to-end gains: coarse Recall@100 improves from 6% to 16.1%, and final Recall@100 after exact reranking increases from 36.5% to 64.3% (Fig. 10).

**(2)  $\alpha$ -correction in candidate reranking.** Enabling  $\alpha$  consistently improves reranking quality across LongBench-V2 splits and candidate ratios, yielding  $\sim +1.5 \text{--} +2.4$  Recall@100 gains while reducing relative inner-product error, with similar improvements on AIME25.

## 5.4. Design Space Exploration

**Parameter choices.** With a fixed budget ( $B \cdot m = 128$ ), we use a compact default ( $B=16$ ,  $m=8$ ,  $K_\omega=256$ ,  $K_r=1$ ) achieving 72.74% recall.

**Multi-tier collision shaping.** A 6-tier bonus expands collision scores from [0, 16] to [0, 96], reducing ties and enabling smaller candidate ratios for the same recall.

**Candidate ratio vs. KV length.** At ratio 0.10, Recall@100 improves from 61.04% (5K) / 67.74% (10K) to 80.36% (30K) / 83.76% (100K), so the required ratio decreases as KV grows.

## 6. Conclusions

We introduced ParisKV, a drift-robust KV-cache retrieval framework that addresses the fundamental challenges of distribution drift and retrieval latency in long-context LLM inference. Our approach is grounded in a key insight: by transforming keys and queries onto a unit hypersphere via normalization and random orthogonal rotation, we can employ data-independent analytic centroids that remain stable regardless of how the key distribution evolves during decoding. This eliminates the centroid staleness that plagues existing methods and maintains high retrieval recall throughout extended generation.

ParisKV employs a GPU-native coarse-to-fine pipeline combining collision-based pruning with calibrated 4-bit reranking, and leverages UVA-based offloading for efficient million-token inference with minimal CPU intervention.

Empirically, ParisKV demonstrates substantial improvements over prior KV-cache retrieval methods. On long-generation reasoning tasks, it improves pass@8 accuracy on AIME25 by +40 to +77 points over PQCache and MagicPIG, while matching or exceeding full attention quality in 7 out of 9 settings. The efficiency gains are equally significant: ParisKV achieves up to  $2.8 \times$  higher decoding throughput

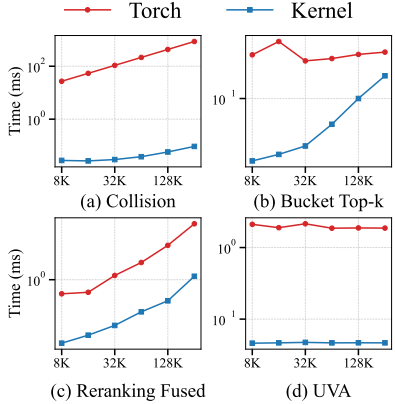


Figure 6. Comparison of runtime between Torch and custom kernels.

Methods	Overall	Short		Medium		Long	
		Easy	Hard	Easy	Hard	Easy	Hard
<i>Qwen3-4B</i>	<b>25.84</b>	27.12	16.53	36.36	25.20	26.67	28.57
PQCache	17.91	16.95	19.00	13.60	19.00	20.00	19.05
MagicPIG	16.70	18.64	10.74	14.77	20.47	28.89	12.70
<b>ParisKV (Ours)</b>	24.60	35.59	19.49	26.14	22.05	28.89	23.81
<i>Qwen-3-8B</i>	<b>33.59</b>	50.85	34.71	32.95	25.98	37.78	28.57
PQCache	25.50	23.70	31.60	28.20	24.00	25.00	20.00
MagicPIG	10.34	8.47	15.70	7.95	7.87	13.33	7.94
<b>ParisKV (Ours)</b>	33.07	52.54	34.71	34.09	26.77	37.21	19.67
<i>DS-R1-Llam-8B</i>	13.12	18.64	15.70	12.50	8.66	11.11	14.29
PQCache	19.90	18.60	21.50	21.60	22.20	15.60	14.30
MagicPIG	13.92	15.25	11.57	11.36	14.17	17.78	17.46
<b>ParisKV (Ours)</b>	<b>28.43</b>	37.29	25.62	28.41	25.20	31.11	30.16

Table 3. LongBench\_V2 accuracy breakdown by context length (Short/Medium/Long) and difficulty (Easy/Hard).

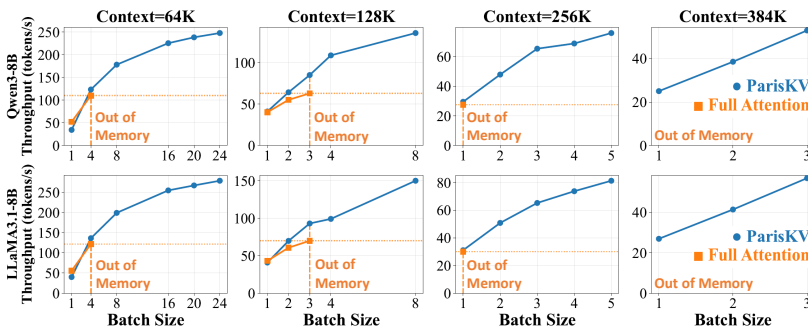


Figure 7. Longbench V2 Decoding throughput vs. Context Length and Batch Size

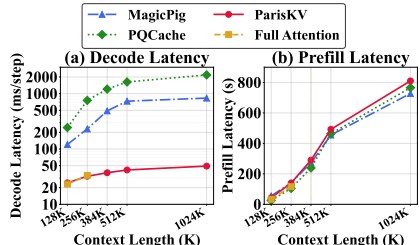


Figure 8. Prefill and Decode Time.

than full attention within its runnable range, and reduces decode latency by  $17\times$  and  $44\times$  compared to MagicPIG and PQCache at million-token scale.

Our results show that carefully designed KV-cache retrieval can simultaneously improve both efficiency and accuracy for long-context inference, even in the presence of drift, opening new possibilities for deploying LLMs in latency-sensitive, long-generation applications.

## Acknowledgements

Supported by EU Horizon projects TwinODIS (101160009), DataGEMS (101188416) and RECITALS (101168490), and by YIAIΩA & NextGenerationEU project HARSH

(YII3TA – 0560901) that is carried out within the framework of the National Recovery and Resilience Plan “Greece 2.0” with funding from the European Union – NextGenerationEU. This work was granted access to the HPC resources of IDRIS under the allocation 2025-A0191012641 made by GENCI.

## Impact Statement

This work improves the efficiency and scalability of KV-cache retrieval for long-context decoding via an algorithm–system co-design that reduces GPU memory pressure and minimizes data movement. These advances can lower the cost and energy of serving long-context language models, enabling wider access to interactive assistants and

long-document applications in research and industry.

At the same time, making long-context inference cheaper and faster may increase the accessibility of high-capacity generative models, which could amplify downstream misuse (e.g., large-scale generation of misleading content) if deployed without safeguards. In addition, KV-cache offloading and on-demand fetching introduce system-level considerations: cached activations may contain information derived from user inputs, so deployments should apply standard privacy and security controls (e.g., access control, isolation between users/tenants, and data retention policies).

We introduce no new training data or model capabilities; our work is purely an inference-time systems optimization. We recommend responsible deployment with existing safety measures, logging and auditing, and privacy-preserving serving practices, especially in multi-tenant settings.

## References

Achiam, J., Adler, S., Agarwal, S., Ahmad, L., Akkaya, I., Aleman, F. L., Almeida, D., Altenschmidt, J., Altman, S., Anadkat, S., et al. Gpt-4 technical report. *arXiv preprint arXiv:2303.08774*, 2023.

Adnan, M., Arunkumar, A., Jain, G., Nair, P. J., Soloveychik, I., and Kamath, P. Keyformer: Kv cache reduction through key tokens selection for efficient generative inference. *Proceedings of Machine Learning and Systems*, 6:114–127, 2024.

Ashkboos, S., Mohtashami, A., Croci, M. L., Li, B., Cameron, P., Jaggi, M., Alistarh, D., Hoefler, T., and Hensman, J. Quarot: Outlier-free 4-bit inference in rotated llms. *Advances in Neural Information Processing Systems*, 37:100213–100240, 2024.

Bai, Y., Tu, S., Zhang, J., Peng, H., Wang, X., Lv, X., Cao, S., Xu, J., Hou, L., Dong, Y., Tang, J., and Li, J. Longbench v2: Towards deeper understanding and reasoning on realistic long-context multitasks. *arXiv preprint arXiv:2412.15204*, 2024.

Balunović, M., Dekoninck, J., Petrov, I., Jovanović, N., and Vechev, M. Matharena: Evaluating llms on uncontaminated math competitions. *Proceedings of the Neural Information Processing Systems Track on Datasets and Benchmark*, 2025.

Cai, Z., Zhang, Y., Gao, B., Liu, Y., Li, Y., Liu, T., Lu, K., Xiong, W., Dong, Y., Hu, J., et al. Pyramidkv: Dynamic kv cache compression based on pyramidal information funneling. *arXiv preprint arXiv:2406.02069*, 2024.

Chen, Y., Zhang, J., Lu, B., Zhang, Q., Zhang, C., Luo, J., Liu, D., Jiang, H., Chen, Q., Liu, J., et al. Retroinfer: A vector-storage approach for scalable long-context llm inference. *arXiv preprint arXiv:2505.02922*, 2025.

Chen, Z., Sadhukhan, R., Ye, Z., Zhou, Y., Zhang, J., Nolte, N., Tian, Y., Douze, M., Bottou, L., Jia, Z., et al. Mag-icpig: Lsh sampling for efficient llm generation. *arXiv preprint arXiv:2410.16179*, 2024.

Dao, T. Flashattention-2: Faster attention with better parallelism and work partitioning. *arXiv preprint arXiv:2307.08691*, 2023.

Dao, T., Fu, D., Ermon, S., Rudra, A., and Ré, C. Flashattention: Fast and memory-efficient exact attention with io-awareness. *Advances in neural information processing systems*, 35:16344–16359, 2022.

Devoto, A., Jeblick, M., and Jégou, S. Expected attention: Kv cache compression by estimating attention from future queries distribution. *arXiv preprint arXiv:2510.00636*, 2025.

Feng, Y., Lv, J., Cao, Y., Xie, X., and Zhou, S. K. Adakv: Optimizing kv cache eviction by adaptive budget allocation for efficient llm inference. *arXiv preprint arXiv:2407.11550*, 2024.

Fu, Y., Cai, Z., Asi, A., Xiong, W., Dong, Y., and Xiao, W. Not all heads matter: A head-level kv cache compression method with integrated retrieval and reasoning. *arXiv preprint arXiv:2410.19258*, 2024.

Gao, Y., Zeng, Z., Du, D., Cao, S., Zhou, P., Qi, J., Lai, J., So, H. K.-H., Cao, T., Yang, F., et al. Seerattention: Learning intrinsic sparse attention in your llms. *arXiv preprint arXiv:2410.13276*, 2024.

Guo, D., Yang, D., Zhang, H., Song, J., Zhang, R., Xu, R., Zhu, Q., Ma, S., Wang, P., Bi, X., et al. Deepseek-r1: Incentivizing reasoning capability in llms via reinforcement learning. *arXiv preprint arXiv:2501.12948*, 2025.

Hendrycks, D., Burns, C., Kadavath, S., Arora, A., Basart, S., Tang, E., Song, D., and Steinhardt, J. Measuring mathematical problem solving with the math dataset. *NeurIPS*, 2021.

Jiang, A. Q., Sablayrolles, A., Mensch, A., Bamford, C., Chaplot, D. S., Casas, D. d. l., Bressand, F., Lengyel, G., Lample, G., Saulnier, L., et al. Mistral 7b. *arXiv preprint arXiv:2310.06825*, 2023.

Jiang, H., Li, Y., Zhang, C., Wu, Q., Luo, X., Ahn, S., Han, Z., Abdi, A. H., Li, D., Lin, C.-Y., et al. Minference 1.0: Accelerating pre-filling for long-context llms via dynamic sparse attention. *Advances in Neural Information Processing Systems*, 37:52481–52515, 2024.

Kim, J.-H., Kim, J., Kwon, S., Lee, J. W., Yun, S., and Song, H. O. Kvzip: Query-agnostic kv cache compression with context reconstruction. *arXiv preprint arXiv:2505.23416*, 2025.

Lai, X., Lu, J., Luo, Y., Ma, Y., and Zhou, X. Flex-prefill: A context-aware sparse attention mechanism for efficient long-sequence inference. *arXiv preprint arXiv:2502.20766*, 2025.

Li, X., Xing, Z., Li, Y., Qu, L., Zhen, H.-L., Liu, W., Yao, Y., Pan, S. J., and Yuan, M. Kvtnet: Sensitivity-aware layer-wise mixed-precision kv cache quantization for efficient and nearly lossless llm inference. *arXiv preprint arXiv:2502.04420*, 2025.

Li, Y., Huang, Y., Yang, B., Venkitesh, B., Locatelli, A., Ye, H., Cai, T., Lewis, P., and Chen, D. Snapkv: Llm knows what you are looking for before generation. *Advances in Neural Information Processing Systems*, 37:22947–22970, 2024.

Lin, H., Xu, H., Wu, Y., Cui, J., Zhang, Y., Mou, L., Song, L., Sun, Z., and Wei, Y. Duquant: Distributing outliers via dual transformation makes stronger quantized llms. *Advances in Neural Information Processing Systems*, 37: 87766–87800, 2024.

Liu, D., Chen, M., Lu, B., Jiang, H., Han, Z., Zhang, Q., Chen, Q., Zhang, C., Ding, B., Zhang, K., et al. Retrievalattention: Accelerating long-context llm inference via vector retrieval. *arXiv preprint arXiv:2409.10516*, 2024a.

Liu, Z., Yuan, J., Jin, H., Zhong, S., Xu, Z., Braverman, V., Chen, B., and Hu, X. Kivi: A tuning-free asymmetric 2bit quantization for kv cache. *arXiv preprint arXiv:2402.02750*, 2024b.

Liu, Z., Zhao, C., Fedorov, I., Soran, B., Choudhary, D., Krishnamoorthi, R., Chandra, V., Tian, Y., and Blankevoort, T. Spinquant: Llm quantization with learned rotations. *arXiv preprint arXiv:2405.16406*, 2024c.

Lu, E., Jiang, Z., Liu, J., Du, Y., Jiang, T., Hong, C., Liu, S., He, W., Yuan, E., Wang, Y., et al. Moba: Mixture of block attention for long-context llms. *arXiv preprint arXiv:2502.13189*, 2025.

Park, J., Jones, D., Morse, M. J., Goel, R., Lee, M., and Lott, C. Keydiff: Key similarity-based kv cache eviction for long-context llm inference in resource-constrained environments. *arXiv preprint arXiv:2504.15364*, 2025.

Qwen Team. Qwen3 technical report. Technical report, 2025. URL <https://arxiv.org/abs/2505.09388>.

Rein, D., Hou, B. L., Stickland, A. C., Petty, J., Pang, R. Y., Dirani, J., Michael, J., and Bowman, S. R. GPQA: A graduate-level google-proof q&a benchmark. In *First Conference on Language Modeling*, 2024.

Sun, H., Chang, L.-W., Bao, W., Zheng, S., Zheng, N., Liu, X., Dong, H., Chi, Y., and Chen, B. Shadowkv: Kv cache in shadows for high-throughput long-context llm inference. *arXiv preprint arXiv:2410.21465*, 2024.

Tang, J., Zhao, Y., Zhu, K., Xiao, G., Kasikci, B., and Han, S. Quest: Query-aware sparsity for efficient long-context llm inference. *arXiv preprint arXiv:2406.10774*, 2024.

Touvron, H., Lavril, T., Izacard, G., Martinet, X., Lachaux, M.-A., Lacroix, T., Rozière, B., Goyal, N., Hambro, E., Azhar, F., et al. Llama: Open and efficient foundation language models. *arXiv preprint arXiv:2302.13971*, 2023.

Xiao, G., Lin, J., Seznec, M., Wu, H., Demouth, J., and Han, S. Smoothquant: Accurate and efficient post-training quantization for large language models. In *International conference on machine learning*, pp. 38087–38099. PMLR, 2023a.

Xiao, G., Tian, Y., Chen, B., Han, S., and Lewis, M. Efficient streaming language models with attention sinks. *arXiv preprint arXiv:2309.17453*, 2023b.

Xiao, G., Tang, J., Zuo, J., Guo, J., Yang, S., Tang, H., Fu, Y., and Han, S. Duoattention: Efficient long-context llm inference with retrieval and streaming heads. *arXiv preprint arXiv:2410.10819*, 2024.

Xu, R., Xiao, G., Huang, H., Guo, J., and Han, S. Xattention: Block sparse attention with antidiagonal scoring. *arXiv preprint arXiv:2503.16428*, 2025.

Yang, A., Li, A., Yang, B., Zhang, B., Hui, B., Zheng, B., Yu, B., Gao, C., Huang, C., Lv, C., et al. Qwen3 technical report. *arXiv preprint arXiv:2505.09388*, 2025.

Yuan, J., Gao, H., Dai, D., Luo, J., Zhao, L., Zhang, Z., Xie, Z., Wei, Y., Wang, L., Xiao, Z., et al. Native sparse attention: Hardware-aligned and natively trainable sparse attention. In *Proceedings of the 63rd Annual Meeting of the Association for Computational Linguistics (Volume 1: Long Papers)*, pp. 23078–23097, 2025.

Zhang, H., Ji, X., Chen, Y., Fu, F., Miao, X., Nie, X., Chen, W., and Cui, B. Pqcache: Product quantization-based kvcache for long context llm inference. *Proceedings of the ACM on Management of Data*, 3(3):1–30, 2025.

Zhang, Z., Sheng, Y., Zhou, T., Chen, T., Zheng, L., Cai, R., Song, Z., Tian, Y., Ré, C., Barrett, C., et al. H2o: Heavy-hitter oracle for efficient generative inference of large language models. *Advances in Neural Information Processing Systems*, 36:34661–34710, 2023.

Zhang, Z., Liu, S., Chen, R., Kailkhura, B., Chen, B., and Wang, Z. Q-hitter: A better token oracle for efficient llm inference via sparse-quantized kv cache. *Proceedings of Machine Learning and Systems*, 6:381–394, 2024.